Atmos. Meas. Tech. Discuss., 3, 5499–5519, 2010
www.atmos-meas-tech-discuss.net/3/5499/2010/
doi:10.5194/amtd-3-5499-2010

Atmospheric Measurement Techniques Discussions

Fast NO_2 retrievals from Odin-OSIRIS limb scatter measurements

A. E. Bourassa[1], **C. A. McLinden**[2], **C. E. Sioris**[2], **S. Brohede**[3], **E. J. Llewellyn**[1], **and D. A. Degenstein**[1]

[1]Institute of Space and Atmospheric Studies, University of Saskatchewan, Saskatchewan, Canada
[2]Environment Canada, Downsview, Ontario, Canada
[3]Department of Radio and Space Science, Chalmers University of Technology, Gotebörg, Sweden

Received: 31 October 2010 – Accepted: 26 November 2010 – Published: 6 December 2010

Correspondence to: A. E. Bourassa (adam.bourassa@usask.ca)

Published by Copernicus Publications on behalf of the European Geosciences Union.

Abstract

The feasibility of retrieving vertical profiles of NO_2 from space-based measurements of limb scattered sunlight has been demonstrated using several different data sets since the 1980's. The NO_2 data product routinely retrieved from measurements made by the Optical Spectrograph and InfraRed Imaging System (OSIRIS) instrument onboard the Odin satellite uses a spectral fitting technique over the 437 to 451 nm range, over which there are 36 individual wavelength measurements. In this work we present a proof of concept technique for the retrieval of NO_2 using only 4 of the 36 OSIRIS measurements in this wavelength range, which reduces the computational cost by almost an order of magnitude. The method is an adaptation of a triplet analysis technique that is currently used for the OSIRIS retrievals of ozone at Chappuis band wavelengths. The results obtained are shown to be in very good agreement with the spectral fit method, and provide an important alternative for two dimensional tomographic algorithms where the computational burden is very high. Additionally this provides a baseline for future instrument design in terms of cost effectiveness and boosting signal to noise by reducing spectral resolution requirements.

1 Introduction

Observations of stratospheric NO_2 began in the 1970's from ground-based zenith-sky measurements (Brewer et al., 1973) and solar occultation from high altitude balloon (Kerr and McElroy, 1976). The pioneering measurement of the stratospheric NO_2 profile from limb scattering geometry actually occurred from space, with the Solar Mesosphere Explorer (Mount et al., 1984). Radiances were measured at two wavelengths of equal NO_2 cross-section, 428.7 and 431.8 nm, or two wavelengths with differing NO_2 cross-section, 439.3 and 442.3 nm (Naudet et al., 1987). Only two wavelengths could be measured per orbit. McElroy (1988) used measurements from balloon limb

AMTD
3, 5499–5519, 2010

scattering geometry at five wavelengths in the 437 to 450 nm range to better account for interfering ozone absorption in the retrieval of NO_2. Recently, measurement of the NO_2 vertical profile by balloon-borne limb scattering was revived by Weidner et al. (2005) who used a spectrometer and retrieved NO_2 by spectral fitting in the 400–450 nm range. Space-based solar occultation measurements of NO_2 were first made by the Stratospheric Aerosol and Gas Experiment (SAGE) II instrument in 1984 (Cunnold et al., 1991).

With the launch of OSIRIS (Llewellyn et al., 2004) on the Odin satellite in 2001 (Murtagh et al., 2002), the information available for the retrieval of NO_2 from space-based limb scatter measurements improved drastically in terms of spectral resolution and range. Sioris et al. (2003) presented the first NO_2 profiles from OSIRIS. Furthermore, Haley et al. (2004) developed a two-step retrieval algorithm for NO_2 relying on differential optical absorption spectroscopy and the maximum a posteriori estimator (see also Haley and Brohede, 2007). Profiles from this algorithm were validated (Brohede et al., 2007b) and used to develop a climatology of stratospheric NO_2 in terms of mean and standard deviation, as a function of latitude, altitude, local solar time and month (Brohede et al., 2007a). The capability of OSIRIS to measure NO_2 in the upper troposphere was best demonstrated by Sioris et al. (2007b), who found that enhancements in NO_2 in this region are predominantly from lightning-generated NO_x. Additionally Sioris et al. (2007a) illustrated Rossby wave breaking with OSIRIS NO_2 near the edge of the Antarctic polar vortex. Recently, Tukiainen et al. (2008) completed the development of the Finnish modified onion-peeling algorithm which determines the ozone profile in a first onion peeling stage and the NO_2 profile in the second iteration.

NO_2 has been retrieved from SCIAMACHY limb scattering measurements operationally by the Germany Aerospace Center (Doicu et al., 2007a,b) and by scientific research groups at universities of Bremen (Eichmann et al., 2004; Rozanov et al., 2005; von Savigny et al., 2005), Harvard (Sioris et al., 2004), and also at the Max Planck Institute for Chemistry (Kühl et al., 2008; Pukite et al., 2010). The measurements of the scientific research groups have been independently validated by Butz et al. (2006). All

AMTD
3, 5499–5519, 2010

of the SCIAMACHY retrievals use a spectral fitting technique over a window of 30 nm or wider in the 420–495 nm range.

The large number of wavelengths measured by current instruments such as OSIRIS, obtained using CCDs or photodiode array detectors, generally leads to greater sensitivity, better precision, and an improved ability to remove interfering signals. Nonetheless, in this work an alternative OSIRIS NO_2 algorithm is presented that uses only a small subset of these wavelengths. An algorithm that can achieve results close to that from the full spectrum is an attractive alternative for several reasons. Instruments based on the diffraction grating and solid-state detector design are expensive, complicated and require a large downlink bandwidth. Their throughput is also limited since optical entrance slits must be narrow to achieve the desired resolution. The addition of a few discrete channels in the NO_2 absorption region is an alternative for instruments designed for high-resolution in other spectral regions, for example, an O_3-BrO-OClO instrument, or for a efficient correction for interference due to NO_2 in an instrument dedicated to another species, such as the Ozone Mapping and Profiling Suite (OMPS) scheduled for launch on the NPP satellite (Flynn et al., 2009). This is also an important alternative to dramatically reduce to the computational time associated with retrievals in a two dimensional tomographic algorithm, where the computational burden is typically very high.

2 The methodology

The retrieval technique we have employed is based on the technique used for space-based limb scatter retrievals of stratospheric ozone in the Chappuis band as discussed in a number of publications including Flittner et al. (2000), von Savigny et al. (2003), Roth et al. (2007) and Degenstein et al. (2009). It is also similar to that used for NO_2 retrievals from the ground-based Brewer MkIV instrument (Cede et al., 2006). In these retrieval schemes, the measurement vector is constructed from a combination of vertical limb scatter radiance profiles at a small number of wavelengths. In this work, we

AMTD
3, 5499–5519, 2010

generalize the previously published "triplet" technique, discussed in the ozone retrieval algorithms referenced above, to use the radiance at 4 strategically chosen wavelengths measured by OSIRIS to construct the measurement vector elements. A Multiplicative Algebraic Reconstruction Technique, which has been successfully used for the retrieval of other species from the OSIRIS measurements (Bourassa et al., 2007; Degenstein et al., 2009), is used to iteratively solve for the NO_2 profile.

2.1 The measurement vector

The construction of the measurement vector relies on the fact that the structure in the NO_2 cross section is relatively broad with respect the 1 nm OSIRIS spectral resolution. A typical NO_2 cross section is shown in the upper panel of Fig. 1 in the spectral window from 437 to 451 nm. This spectral range is used in the official OSIRIS version 3.0 NO_2 data product, which is based on the spectral fitting technique presented in Haley et al. (2004) and Haley and Brohede (2007). The lower panel of Fig. 1 shows the spectrum measured by OSIRIS along a line of sight tangent at 25 km altitude. For illustrative purposes, this spectrum has been normalized in a wavelength-by-wavelength sense with a spectrum measured along a line of sight tangent at 45 km altitude. Each of the 36 OSIRIS pixels in this window are marked by x's on the spectrum, all of which are used in the spectral fitting technique for the official version 3.0 data product. In this work, we have strategically chosen 4 OSIRIS pixels as a minimum set of wavelengths to use for an NO_2 retrieval. These are indicated by the circles in each plot.

The familiar form of the typical triplet measurement vector, as commonly used in the retrievals of ozone from limb scattered sunlight noted above, is defined as

$$\boldsymbol{y}_j = \ln\left(\frac{\sqrt{I_j(\lambda_1)\, I_j(\lambda_2)}}{I_j(\lambda_3)}\right). \quad (1)$$

In this equation the measurement vector element $\boldsymbol{y}_j$, that corresponds to a tangent altitude denoted by the subscript j, is calculated using three radiance measurements, two

AMTD
3, 5499–5519, 2010

of which are reference wavelengths that are typically weakly absorbing (λ_1 and λ_2), and a third at a strongly absorbing wavelength (λ_3). Equation (1) can written equivalently as

$$\boldsymbol{y}_j = 0.5 \ln\left(I_j(\lambda_1)\right) + 0.5 \ln\left(I_j(\lambda_2)\right) - 1.0 \ln\left(I_j(\lambda_3)\right). \quad (2)$$

This form of the triplet measurement vector is also common in the literature and is relevant to this work. In this form, there is a coefficient that multiplies the natural log of each radiance measurement, i.e. 0.5, 0.5 and −1.0. Positive coefficients scale the reference or weakly absorbing wavelengths and negative coefficients scale the absorbing wavelength. Also, the sum of all coefficients is identically zero, as the reference wavelength coefficients sum to 1.0 and the absorbing wavelength coefficients sum to −1.0.

Following this logic, Eq. (2) can be generalized for n radiance measurements and written as,

$$\boldsymbol{y}_j = p_1 \ln\left(I_j(\lambda_1)\right) + p_2 \ln\left(I_j(\lambda_2)\right) + \ldots - q_1 \ln\left(I_j(\lambda_m)\right) - q_2 \ln\left(I_j(\lambda_{m+1})\right) - \ldots, \quad (3)$$

where wavelengths 1 to $m-1$ are the reference wavelengths and the coefficients

$$\sum_i p_i = 1, \quad (4)$$

and wavelengths m to n are the absorbing wavelengths and

$$\sum_i q_i = -1, \quad (5)$$

such that the sum over all coefficients is zero.

The measurement vector used in this work is constructed using four radiance measurements. Three of these are weakly absorbing reference wavelengths: $\lambda_1 = 447.04$ nm, $\lambda_2 = 449.81$ nm and $\lambda_3 = 450.21$ nm and are located at local minimums in the cross section as shown in Fig. 1. A single absorbing wavelength, $\lambda_4 = 448.23$ nm,

AMTD
3, 5499–5519, 2010

is located at the local maximum of the cross section. The measurement vector is constructed as

$$\boldsymbol{y}_j = 0.5 \ln\left(I_j(\lambda_1)\right) + 0.25 \ln\left(I_j(\lambda_2)\right) + 0.25 \ln\left(I_j(\lambda_3)\right) - 1.0 \ln\left(I_j(\lambda_4)\right). \quad (6)$$

This effectively states that the measurement is the difference of the weighted average of the log of the radiance at the three reference wavelengths and the log of the wavelength at the local peak in the NO_2 cross section. These wavelengths are strategically chosen so as to maximize the sensitivity to NO_2 with a very small subset of radiance measurements. As with the triplet technique, the reference wavelengths are chosen on either side of the absorption feature. With the absorbing wavelength at the peak, the triplet effectively is a measure of the depth of the absorption. We have chosen to add a fourth wavelength so as to increase the number of measurements and systematically reduce the effect of random noise. However, using wavelengths between the local maximum and minimum values of the absorption feature, i.e. within the feature, serves only to reduce the sensitivity of the measurement vector. For example, if multiple wavelengths around the peak were incorporated into the measurement vector, the effective depth of the absorption feature is decreased through the averaging. Thus because the minimum in the cross section is relatively wide on the long wavelength side of the absorption feature, we can add an additional reference wavelength without decreasing the effective depth. These two reference wavelengths on the short side of the absorption peak are averaged with equal weight with respect to the reference on the long side of the peak.

The normalization technique

Typically, measurement vector elements for limb scatter retrievals are normalized by a measurement at a higher tangent altitude. This removes the requirement for an absolute calibration and decreases systematic effects due to uncertainty in forward model parameters such as the effective reflectance or albedo term (see for example von Savigny et al., 2003). For this work we have not used a direct division by higher

AMTD
3, 5499–5519, 2010

tangent altitude measurements. As shown in Eq. (6) the radiance at each tangent height is used directly. For a typical OSIRIS scan, the result of applying Eq. (6) is shown in the left hand panel of Fig. 2. In this case, the measurement vector approaches a constant non-zero value at high tangent altitude. Fluctuations about this value are due to measurement noise. By definition, a normalized measurement vector is identically zero at the normalization altitude as each term simplifies to the logarithm of 1.0. Due to this logarithmic nature of the measurement vector, the normalization can be viewed as an offset term, constant with tangent altitude, that drives the measurement vector to zero at the normalization altitude.

Since the radiances at high tangent altitude can contain significant noise due to decreasing limb signal, the noise in a single measurement used for normalization can systematically affect the entire profile as it results in an offset of the measurement vector. For this reason, rather than normalize with a single measurement, we calculate the average value of the measurement vector over a range of high tangent altitudes and then offset the entire measurement vector, in a negative sense, by that average value. The overall effect is similar to a high altitude normalization and the measurement vector approaches zero at high tangent altitude; however, the impact of noise is reduced by using multiple measurements. This is shown in the right panel of Fig. 2, where the normalization range includes all measurements used to construct the average value used for the offset.

This same procedure is applied to the measured and the modelled vectors during the retrieval process. It has almost no impact on computational efficiency of the algorithm as the vast majority of computation time is spent forward modelling the radiance profiles for different wavelengths; additional lines of sight at a given wavelength require almost no additional computational time.

AMTD
3, 5499–5519, 2010

2.2 The MART inversion

The Multiplicative Algebraic Reconstruction Technique (MART) equation, used to iteratively update the state parameter based on the forward modelled measurement vector,

$$x_i^{(n+1)} = x_i^{(n)} \sum_j \left(\frac{y_j^{\text{measured}}}{y_j^{\text{modelled}}} W_{ji} \right), \quad (7)$$

has been described in application to limb scatter in many previous publications (see for example Roth et al., 2007; Bourassa et al., 2007; Degenstein et al., 2009). It has also been used to retrieve 1.27 µm Oxygen InfraRed Atmospheric Band emissions in the mesosphere (Degenstein et al., 2003). The application of this equation is straight forward. The ratio of the measured and modelled measurement vector $\boldsymbol{y}_j$, where j indicates tangent altitude, it is used to retrieve a the state parameter vector $\boldsymbol{x}_i$, where the i indicates altitude. Of course in this case, $\boldsymbol{x}_i$ is the vertical profile of NO_2.

In this work, three measurement vector elements are considered important to the retrieval at any given altitude, i. These are the measurement vector elements corresponding to tangent altitudes through the spherical shell at altitude i and the next two lower tangent altitude vector elements. These two measurements have significant path lengths through the shell at altitude i on the near and far sides of the tangent point. The weights W_{ij} associated with these three vector elements are 0.5, 0.3 and 0.2 where the weight decreases with decreasing tangent altitude. For a full discussion of this see Bourassa et al. (2007)

A photochemical box model is used to generate the initial guess profile. This is the same profile that is used as the apriori profile for the optimal estimation retrieval used for the spectral fitting in the official version 3.0 product (Brohede et al., 2007a). The SASKTRAN model (Bourassa et al., 2008), which is a spherical successive orders radiative transfer code, is used for the forward model in this work. The measurement vector for a typical scan and the last 10 of 15 iterations of the retrieval are shown in Fig. 3.

AMTD
3, 5499–5519, 2010

3 Results

The results from the retrieval using the methodology outlined above can be directly compared with the official OSIRIS version 3.0 NO_2 data product. As a proof of concept for the purposes of this work a typical full day of OSIRIS measurements is analyzed. This is the illuminated portion of 16 full orbits of measurements. On 22 April 2002, the sunlit portion of the Odin orbit covers almost the entire northern hemisphere. The ascending node of the orbit is at local dusk; as the satellite passes over the northernmost part of the orbit, the time is local noon. The descending node is at local dawn. As NO_2 is photochemically active, the comparisons between the two methods must be done such that local time is synchronized for all retrievals going into a single average.

Figure 4 shows the comparison between the official OSIRIS version 3.0 NO_2 retrievals, which use the entire spectral window, and those calculated using the methodology outlined above using the radiance at the 4 indicated wavelengths. The upper panel shows our results for measurements collected only on the descending node or morning twilight node of the Odin orbit. All retrievals for the 16 orbits on 22 April 2002, are binned in 10° of latitude. The northernmost bin contains only data from 80 to 82° as the inclination of the Odin orbit is 98°. Recall that the Odin orbit is such that the low latitude bins represent measurements made at local dawn and the most northern bins represent data collected near local noon. A rapid sweep between local times occurs around 70° latitude. The middle panel of Fig. 4 shows the same but for the OSIRIS version 3.0 retrieval. The comparison is qualitatively very good and on average there are very few differences between the values as retrieved from identical radiance measurements but with vastly different techniques.

The lower panel of Fig. 4 shows the percent difference between the results shown in the upper two panels. The percent difference is determined as the difference between our results minus the official version divided by the average of the two expressed as a percentage. Only at the altitude extremes is there any significant difference between the results obtained from the two methods. The upper two panels of this figure show

AMTD
3, 5499–5519, 2010

how the peak altitude of the NO_2 profile decreases in altitude as latitude increases or as the local time progresses. Generally, the percent difference between the two methods is less than 10% near the peak of the NO_2 number density profile. There is one region of interest on the these panels; at high latitudes where the peak of the NO_2 profile is at a lower altitude and a higher absolute value the two methods produce somewhat different values. Below the peak of the NO_2 layer our retrievals are consistently up to 25% lower than those of the official data product. The reason for this discrepancy has not been determined.

As a further illustration of the quality of the data retrieved using this technique Fig. 5 shows the mean vertical profiles taken from the upper two panels of Fig. 4, and additionally mean profiles from the ascending track, or evening twilight, part of the Odin orbits. Also included on this figure are the initial guess for the MART technique, which as mentioned previously is the apriori for the version 3.0 retrievals. For all latitudes and local time conditions there is good agreement between the results retrieved using the two different methods. However, the high latitude discrepancy is also apparent in these plots on both the ascending and descending tracks of the orbit.

4 Conclusions

The retrievals of NO_2 produced by the technique outlined here, using radiances measured at 4 wavelengths, compare very well with those obtained by the official OSIRIS version 3.0 product, which uses 36 wavelengths in a spectral fitting inversion. The computation time required for our retrievals is reduced by almost an order of magnitude providing a viable alternative method for tomographic inversion or as a fast and self consistent correction for NO_2 as an interfering species in a measurement and retrieval focused on another species.

AMTD
3, 5499–5519, 2010

Acknowledgements. This work was supported by the Natural Sciences and Engineering Research Council (Canada) and the Canadian Space Agency. Odin is a Swedish-led satellite project funded jointly by Sweden (SNSB), Canada (CSA), France (CNES) and Finland (Tekes).

References

Bourassa, A. E., Degenstein, D. A., Gattinger, R. L., and Llewellyn, E. J.: Stratospheric aerosol retrieval with OSIRIS limb scatter measurements, J. Geophys. Res., 112, D10217, doi:10.1029/2006JD008079, 2007. 5503, 5507

Bourassa, A. E., Degenstein, D. A., and Llewellyn, E. J.: SASKTRAN: A spherical geometry radiative transfer code for efficient estimation of limb scattered sunlight, J. Quant. Spectros. Ra., 109, 52–73, 2008. 5507

Brewer, A. W., McElroy, C. T., and Kerr, J. B.: Nitrogen Dioxide concentrations in the atmosphere, Nature, 246, 129–133, doi:10.1038/246129a0, 1973. 5500

Brohede, S., McLinden, C. A., Berthet, G., Haley, C. S., Murtagh, D., and Sioris, C. E.: A stratospheric NO_2 climatology from Odin/OSIRIS limb-scatter measurements, Can. J. Phys., 85, 1253–1274, doi:10.1139/P07-141, 2007a. 5501, 5507

Brohede, S. M., Haley, C. S., McLinden, C. A., Sioris, C. E., Murtagh, D. P., Petelina, S. V., Llewellyn, E. J., Bazureau, A., Goutail, F., Randall, C. E., Lumpe, J. D., Taha, G., Thomasson, L. W., and Gordley, L. L.: Validation of Odin/OSIRIS stratospheric NO_2 profiles, J. Geophys. Res., 112, D07310, doi:10.1029/2006JD007586, 2007b. 5501

Butz, A., Bösch, H., Camy-Peyret, C., Chipperfield, M., Dorf, M., Dufour, G., Grunow, K., Jeseck, P., Kühl, S., Payan, S., Pepin, I., Pukite, J., Rozanov, A., von Savigny, C., Sioris, C., Wagner, T., Weidner, F., and Pfeilsticker, K.: Inter-comparison of stratospheric O_3 and NO_2 abundances retrieved from balloon borne direct sun observations and Envisat/SCIAMACHY limb measurements, Atmos. Chem. Phys., 6, 1293–1314, doi:10.5194/acp-6-1293-2006, 2006. 5501

Cede, A., Herman, J., Richter, A., Krotkov, N., and Burrows, J.: Measurements of nitrogen dioxide total column amounts using a Brewer double spectrophotometer in direct Sun mode, J. Geophys. Res., 111, D05304, doi:10.1029/2005JD006585, 2006. 5502

Cunnold, D. M., Zawodny, J. M., Chu, W. P., McCormick, M. P., Pommereau, J. P., and Goutail, F.: Validation of SAGE II NO_2 measurements, J. Geophys. Res., 96, 12913–12925, doi:10.1029/91JD01344, 1991. 5501

AMTD
3, 5499–5519, 2010

Degenstein, D. A., Llewellyn, E. J., and Lloyd, N. D.: Volume emission rate tomography from a satellite platform, Appl. Optics, 42, 1441–1450, 2003. 5507

Degenstein, D. A., Bourassa, A. E., Roth, C. Z., and Llewellyn, E. J.: Limb scatter ozone retrieval from 10 to 60 km using a multiplicative algebraic reconstruction technique, Atmos. Chem. Phys., 9, 6521–6529, doi:10.5194/acp-9-6521-2009, 2009. 5502, 5503, 5507

Doicu, A., Hilgers, S., von Bargen, A., Rozanov, A., Eichmann, K., von Savigny, C., and Burrows, J. P.: Information operator approach and iterative regularization methods for atmospheric remote sensing, J. Quant. Spect. Ra., 103, 340–350, doi:10.1016/j.jqsrt.2006.05.002, 2007a. 5501

Doicu, A., Schreier, S., Hilgers, S., and Hess, M.: Error analysis and minimum bound method for atmospheric remote sensing, Environ. Modell. Softw., 22, 837–846, doi:10.1016/j.envsoft.2005.08.006, 2007b. 5501

Eichmann, K., Kaiser, J. W., von Savigny, C., Rozanov, A., Rozanov, V. V., Bovensmann, H., von König, M., and Burrows, J. P.: SCIAMACHY limb measurements in the UV/Vis spectral region: first results, Adv. Space Res., 34, 775–779, doi:10.1016/j.asr.2003.05.057, 2004. 5501

Flittner, D. E., Bhartia, P. K., and Herman, B. M.: O_3 profiles retrieved from limb scatter measurements: Theory, Geophys. Res. Lett., 27, 2601–2604, doi:10.1029/1999GL011343, 2000. 5502

Haley, C. S. and Brohede, S.: Status of the Odin/OSIRIS stratospheric O_3 and NO_2 data products, Can. J. Phys., 85, 1177–1194, doi:10.1139/P07-114, 2007. 5501, 5503

Haley, C. S., Brohede, S. M., Sioris, C. E., Griffioen, E., Murtagh, D. P., McDade, I. C., Eriksson, P., Llewellyn, E. J., Bazureau, A., and Goutail, F.: Retrieval of stratospheric O_3 and NO_2 profiles from Odin Optical Spectrograph and Infrared Imager System (OSIRIS) limb-scattered sunlight measurements, J. Geophys. Res., 109, D16303, doi:10.1029/2004JD004588, 2004. 5501, 5503

Kerr, J. B. and McElroy, C. T.: Measurment of Stratospheric Nitrogen Dioxide from the AES Stratospheric Balloon Program, Atmosphere, 14, 166–171, 1976. 5500

Kühl, S., Pukite, J., Deutschmann, T., Platt, U., and Wagner, T.: SCIAMACHY limb measurements of NO_2, BrO and OClO. Retrieval of vertical profiles: Algorithm, first results, sensitivity and comparison studies, Adv. Space Res., 42, 1747–1764, doi:10.1016/j.asr.2007.10.022, 2008. 5501

AMTD
3, 5499–5519, 2010

Llewellyn, E. J., Lloyd, N. D., Degenstein, D. A., Gattinger, R. L., Petelina, S. V., Bourassa, A. E., Wiensz, J. T., Ivanov, E. V., McDade, I. C., Solheim, B. H., McConnell, J. C., Haley, C. S., von Savigny, C., Sioris, C. E., McLinden, C. A., Griffioen, E., Kaminski, J., Evans, W. F., Puckrin, E., Strong, K., Wehrle, V., Hum, R. H., Kendall, D. J. W., Matsushita, J., Murtagh, D. P., Brohede, S., Stegman, J., Witt, G., Barnes, G., Payne, W. F., Piché, L., Smith, K., Warshaw, G., Deslauniers, D.-L., Marchand, P., Richardson, E. H., King, R. A., Wevers, I., McCreath, W., Kyrölä, E., Oikarinen, L., Leppelmeier, G. W., Auvinen, H., Mégie, G., Hauchecorne, A., Lefèvre, F., de La Nöe, J., Ricaud, P., Frisk, U., Sjoberg, F., von Schéele, F., and Nordh, L.: The OSIRIS instrument on the Odin spacecraft, Can. J. Phys., 82, 411–422, 2004. 5501

McElroy, C. T.: Stratospheric nitrogen dioxide concentrations as determined from limb brightness measurements made on 17 June 1983, J. Geophys. Res., 93, 7075–7083, doi:10.1029/JD093iD06p07075, 1988. 5500

Mount, G. H., Rusch, D. W., Zawodny, J. M., Barth, C. A., and Noxon, J. F.: Measurements of stratospheric NO_2 from the Solar Mesosphere Explorer satellite, I – An overview of the results, J. Geophys. Res., 89, 1327–1340, doi:10.1029/JD089iD01p01327, 1984. 5500

Murtagh, D., Frisk, U., Merino, F., Ridal, M., Jonsson, A., Stegman, J., Witt, G., Eriksson, P., Jiménez, C., Megie, G., de La Noë, J., Ricaud, P., Baron, P., Pardo, J. R., Hauchcorne, A., Llewellyn, E. J., Degenstein, D. A., Gattinger, R. L., Lloyd, N. D., Evans, W. F. J., McDade, I. C., Haley, C. S., Sioris, C., von Savigny, C., Solheim, B. H., McConnell, J. C., Strong, K., Richardson, E. H., Leppelmeier, G. W., Kyrölä, E., Auvinen, H., and Oikarinen, L.: Review: An overview of the Odin atmospheric mission, Can. J. Phys., 80, 309–319, 2002. 5501

Naudet, J. P., Rusch, D. W., Thomas, R. J., Clancy, R. T., Barth, C. A., Wedding, J., Zawodny, J. M., Fabian, P., and Helten, M.: Stratopsheric NO_2 from the Solar Mesosphere Explorer during MAP/GLOBUS 1983, Planet. Space Sci., 35, 631–635, doi:10.1016/0032-0633(87)90129-2, 1987. 5500

Pukite, J., Kühl, S., Deutschmann, T., Dörner, S., Jöckel, P., Platt, U., and Wagner, T.: The effect of horizontal gradients and spatial measurement resolution on the retrieval of global vertical NO_2 distributions from SCIAMACHY measurements in limb only mode, Atmos. Meas. Tech., 3, 1155–1174, doi:10.5194/amt-3-1155-2010, 2010. 5501

Roth, C. Z., Degenstein, D. A., Bourassa, A. E., and Llewellyn, E. J.: The retrieval of vertical profiles of the ozone number density using Chappuis band absorption information and a multiplicative algebraic reconstruction technique, Can. J. Phys., 85, 1225–1243, doi:10.1139/P07-130, 2007. 5502, 5507

AMTD
3, 5499–5519, 2010

Rozanov, A., Bovensmann, H., Bracher, A., Hrechanyy, S., Rozanov, V., Sinnhuber, M., Stroh, F., and Burrows, J. P.: NO_2 and BrO vertical profile retrieval from SCIAMACHY limb measurements: Sensitivity studies, Adv. Space Res., 36, 846–854, doi:10.1016/j.asr.2005.03.013, 2005. 5501

Sioris, C. E., Haley, C. S., McLinden, C. A., von Savigny, C., McDade, I. C., McConnell, J. C., Evans, W. F. J., Lloyd, N. D., Llewellyn, E. J., Chance, K. V., Kurosu, T. P., Murtagh, D., Frisk, U., Pfeilsticker, K., Bösch, H., Weidner, F., Strong, K., Stegman, J., and Mégie, G.: Stratospheric profiles of nitrogen dioxide observed by Optical Spectrograph and Infrared Imager System on the Odin satellite, J. Geophys. Res., 108(D7), 4215, doi:10.1029/2002JD002672, 2003. 5501

Sioris, C. E., Kurosu, T. P., Martin, R. V., and Chance, K.: Stratospheric and tropospheric NO_2 observed by SCIAMACHY: first results, Adv. Space Res., 34, 780–785, doi:10.1016/j.asr.2003.08.066, 2004. 5501

Sioris, C. E., Chabrillat, S., McLinden, C. A., Haley, C. S., Rochon, Y. J., Ménard, R., Charron, M., and McElroy, C. T.: OSIRIS observations of a tongue of NOx in the lower stratosphere at the Antarctic vortex edge: comparison with a high-resolution simulation from the Global Environmental Multiscale (GEM) model, Can. J. Phys., 85, 1195–1207, doi:10.1139/P07-123, 2007a. 5501

Sioris, C. E., McLinden, C. A., Martin, R. V., Sauvage, B., Haley, C. S., Lloyd, N. D., Llewellyn, E. J., Bernath, P. F., Boone, C. D., Brohede, S., and McElroy, C. T.: Vertical profiles of lightning-produced NO_2 enhancements in the upper troposphere observed by OSIRIS, Atmos. Chem. Phys., 7, 4281–4294, doi:10.5194/acp-7-4281-2007, 2007b. 5501

Tukiainen, S., Hassinen, S., Seppälä, A., Auvinen, H., Kyrölä, E., Tamminen, J., Haley, C. S., Lloyd, N., and Verronen, P. T.: Description and validation of a limb scatter retrieval method for Odin/OSIRIS, J. Geophys. Res., 113, D04308, doi:10.1029/2007JD008591, 2008. 5501

von Savigny, C., Haley, C. S., Sioris, C. E., McDade, I. C., Llewellyn, E. J., Degenstein, D., Evans, W. F. J., Gattinger, R. L., Griffioen, E., Kyrölä, E., Lloyd, N. D., McConnell, J. C., McLinden, C. A., Mégie, G., Murtagh, D. P., Solheim, B., and Strong, K.: Stratospheric ozone profiles retrieved from limb scattered sunlight radiance spectra measured by the OSIRIS instrument on the Odin satellite, Geophys. Res. Lett., 30, 8, doi:10.1029/2002GL016401, 2003. 5502, 5505

AMTD
3, 5499–5519, 2010

von Savigny, C., McDade, I. C., Griffioen, E., Haley, C. S., Sioris, C. E., and Llewellyn, E. J.: Sensitivity studies and first validation of stratospheric ozone profile retrievals from Odin/OSIRIS observations of limb-scattered solar radiation, Can. J. Phys., 83, 957–972, 2005. 5501

Weidner, F., Bösch, H., Bovensmann, H., Burrows, J. P., Butz, A., Camy-Peyret, C., Dorf, M., Gerilowski, K., Gurlit, W., Platt, U., von Friedeburg, C., Wagner, T., and Pfeilsticker, K.: Balloon-borne limb profiling of UV/vis skylight radiances, O_3, NO_2, and BrO: technical set-up and validation of the method, Atmos. Chem. Phys., 5, 1409–1422, doi:10.5194/acp-5-1409-2005, 2005. 5501

AMTD
3, 5499–5519, 2010

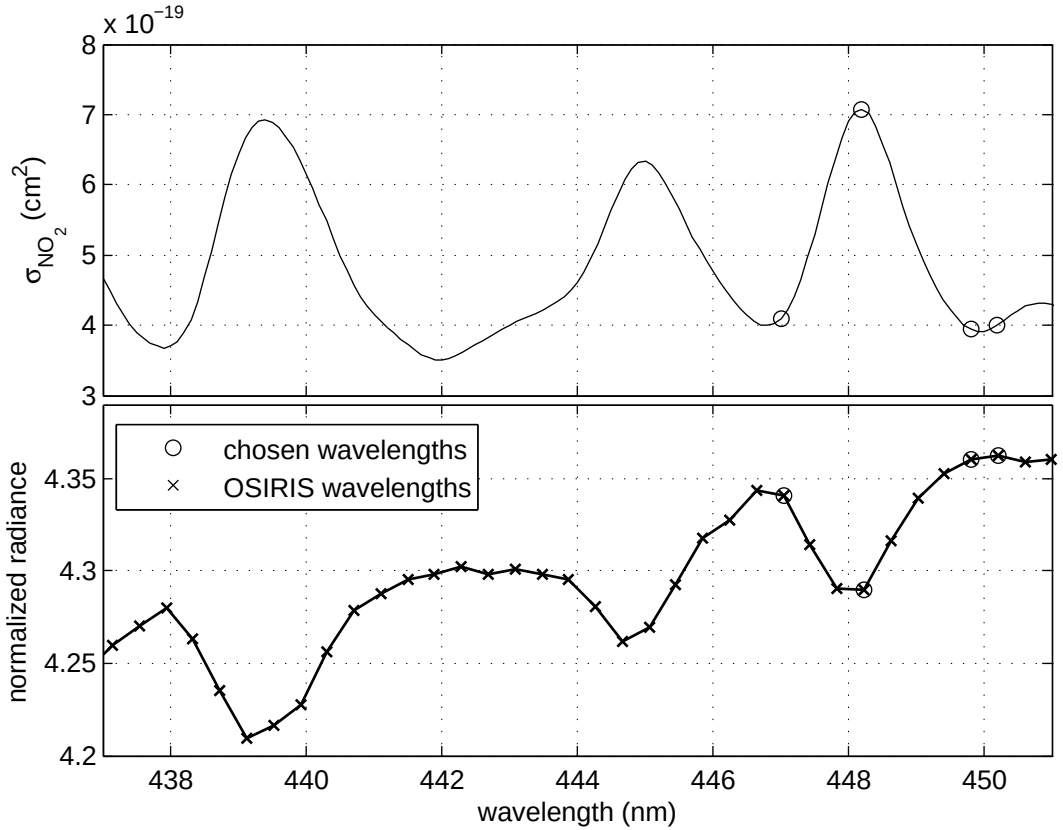

Fig. 1. The NO_2 cross section and the measured OSIRIS spectrum in the wavelength range from 437 nm to 451 nm. The 4 wavelengths used in this technique are indicated with circle markers at the long wavelength end. The lower panel shows an OSIRIS 23 km tangent altitude spectrum in the same wavelength range after it has been normalized by the OSIRIS spectrum measured along a 45 km tangent altitude line of sight. OSIRIS pixels are indicated with x markers.

AMTD
3, 5499–5519, 2010

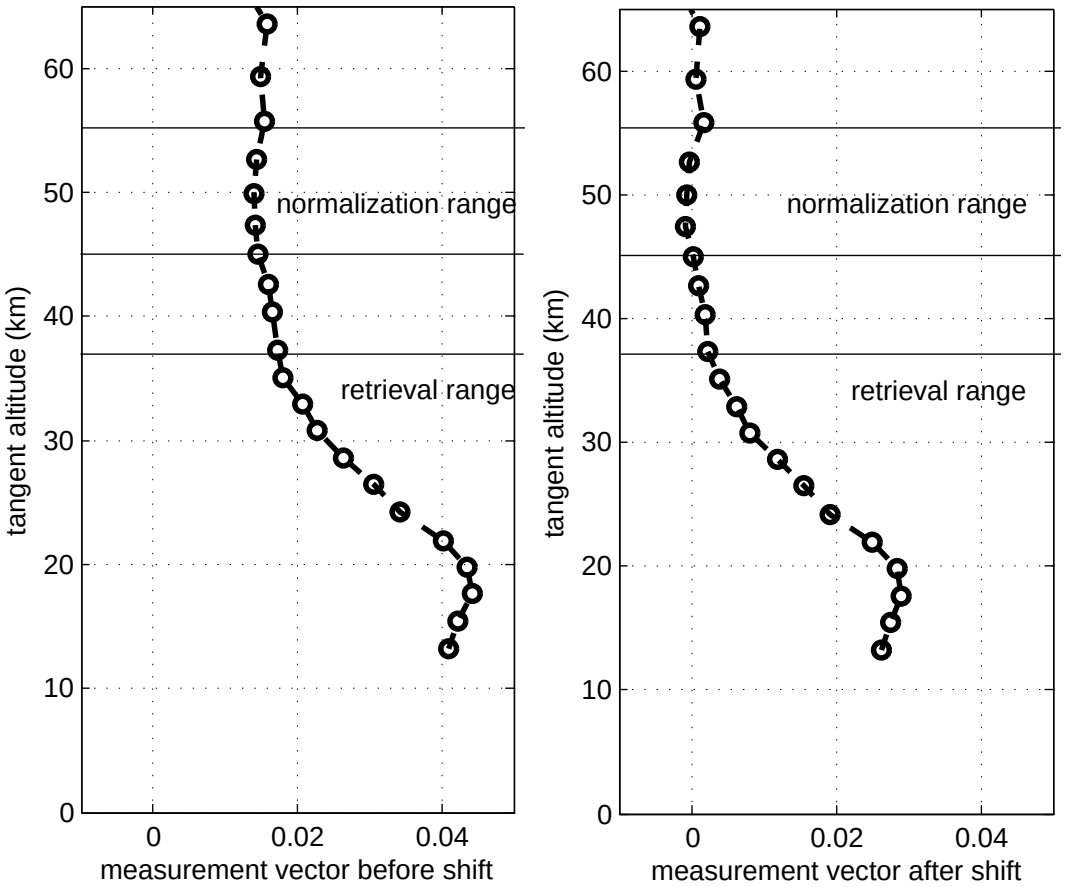

Fig. 2. The measurement vectors. The vector shown in the left hand panel is calculated using Eq. (6). The vector shown in the right hand panel is shifted by a constant such that the average value is zero over the normalization range.

AMTD
3, 5499–5519, 2010

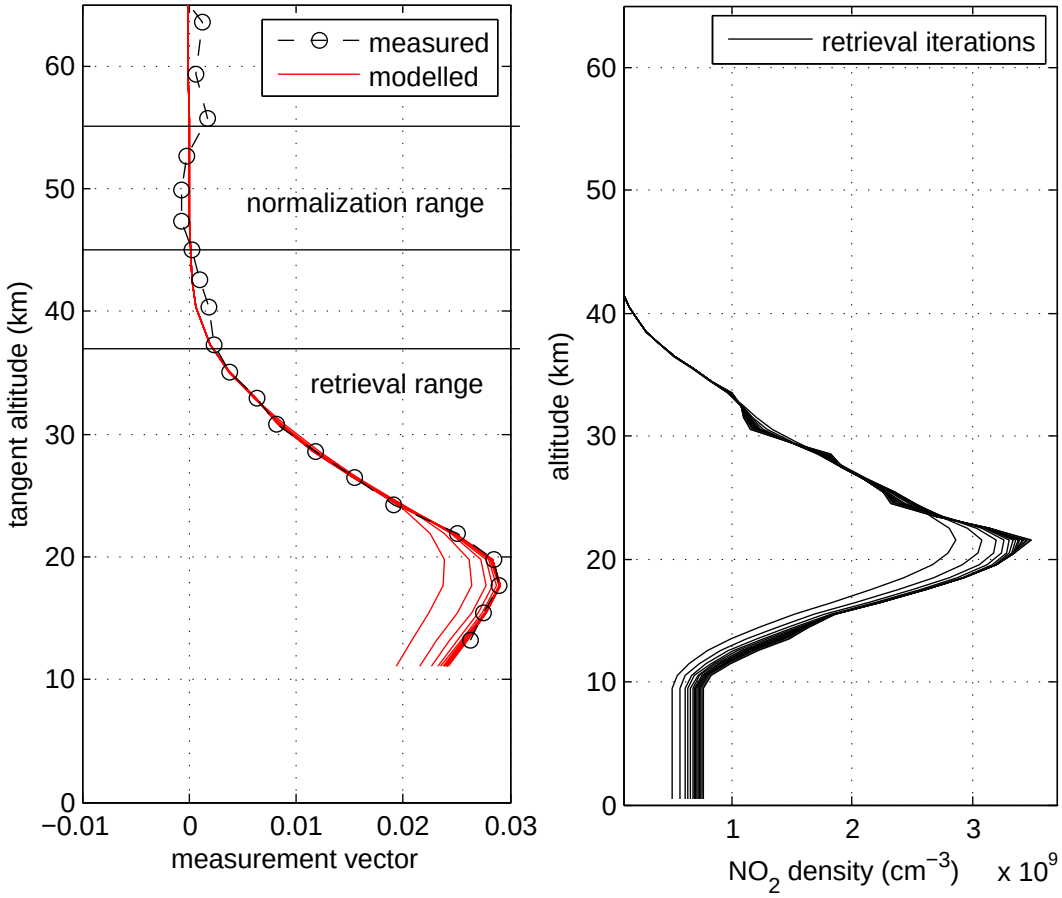

Fig. 3. The convergence of the measurement vector and the retrieved NO_2 profile. The left panel shows the measured vector and its modelled value for the last 10 of 15 iterations of the retrieval. Also indicated in this panel are the range over which the vector is normalized and the range over which the NO_2 is retrieved.

AMTD
3, 5499–5519, 2010

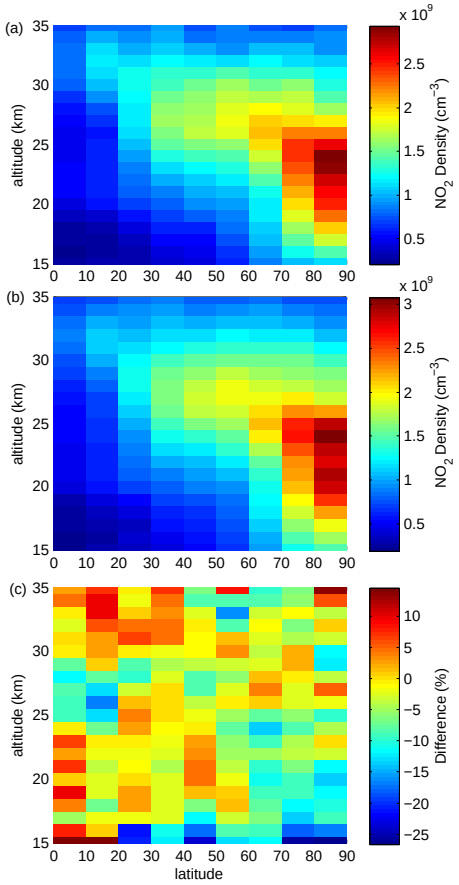

Fig. 4. A daily average of our retrievals (top) compared with the official OSIRIS version 3.0 retrievals (middle). In this plot only data collected during the descending node of the Odin orbit, i.e. measurements at local morning twilight, are presented. The bottom panel is the percent difference between the two retrieved data sets.

AMTD
3, 5499–5519, 2010

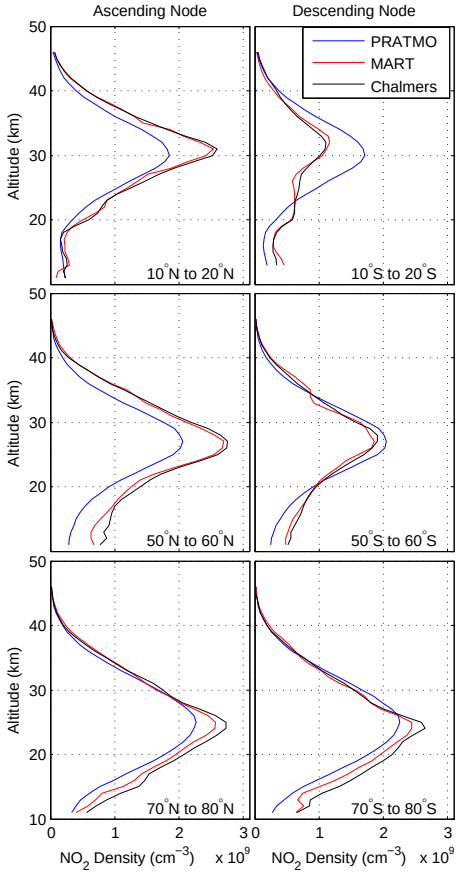

Fig. 5. Selected zonal mean profiles from one day of OSIRIS measurements. Each panel compares the zonal average of our retrievals and the official OSIRIS version 3.0 product. Included in each panel is the zonal average of the apriori/initial guess profile (labeled PRATMO).

AMTD
3, 5499–5519, 2010